

# ASSESSMENT OF FATIGUE STRENGTH OF LOW ALLOY STEELS FOR SHIPS' CRANKSHAFT

S. Omata and H. Matsushita

Research Institute, Nippon Kaiji Kyokai, 1-8-3, Ohnodai, Midori-Ku, Chiba, Japan

## ABSTRACT

Rotational bending fatigue tests for low alloy steels, KSFA80, KSFA110 were carried out to clarify the property of fatigue strength of high tensile forged materials. Fatigue fractures occurred even though the repeated stress exceeded  $10^8$  cycles, which started at an interior inclusion. Fatigue strength of forged materials show anisotropy depending on the relative direction of specimen to forged fiber flow, and it is shown that this anisotropy of fatigue strength is due to the projective shape and size of inclusions at crack origin to a plain perpendicular to the maximum stress direction. The effect of non-metallic inclusion to fatigue strength was estimated using the *area* parameter model.

## KEYWORDS

High cycle fatigue, Low alloy steel, Forged steel, Crankshaft, Inclusion, Interior fracture.

## INTRODUCTION

Recent years, the use of low alloy steels as material for crankshafts has gained for small and medium sized diesel engines, because of a demand for engines to be smaller and lighter in weight. Generally, fatigue design of products is based on the fatigue limit defined at  $10^7$  cycles of repeated stress, but for high speed engines,  $10^7$  cycles will be achieved in a short time and can not be enough to evaluate the fatigue limit. Therefore, the necessity for understanding the fatigue strength characteristic in the long life range of more than  $10^7$  cycles is recognized. But the fatigue data of low-alloy steels in the long life range are not enough under the present situation. In this study, fatigue tests of low alloy steels up to  $10^8$  cycles or more of repeated stress were performed to clarify the fatigue properties in the long life range. On the other hand, fatigue strength of forged products, like CGF (Continuous Grain Flow) crankshaft, are affected by the differences in the angle of the direction of applied stress and the direction of forged fiber flow, because fatigue strength of forged steels show anisotropy depending on the relative direction to the forged fiber flow. In this study, the effect of relationship between forged fiber flow and the direction of applied stress, and the effect of shape and size of inclusions in materials to fatigue strength were examined.

## EXPERIMENTAL DETAILS

Four types of materials were subjected to fatigue testing, two types of KSFA80 and two types of KSFA110 (Class NK standards). The chemical compositions of each sample material are shown in table 1 and the

forging ratio and the heat treatment conditions are shown in table 2.

**TABLE 1**  
CHEMICAL COMPOSITION OF MATERIALS

Material	C	Si	Mn	P	S	Ni	Cr	Mo	Cu
KSFA80A	0.43	0.26	0.73	0.011	0.005	0.44	1.07	0.22	0.08
KSFA80B	0.44	0.30	0.74	0.010	0.003	0.51	1.10	0.25	0.04
KSFA110A	0.37	0.27	0.40	0.009	0.003	2.82	1.61	0.41	0.05
KSFA110B	0.33	0.26	0.51	0.014	0.003	2.99	3.00	0.61	0.03

**TABLE 2**  
FORGING RATIO AND CONDITIONS OF HEAT TREATMENT

Material	Forging ratio	Heat Treatment
KSFA80A	3.2S	870°C • 9Hr OilQuenching & 640°C 15Hr AirCooling
KSFA80B	11.9S	870°C • 9Hr OilQuenching & 635°C 20Hr FurnaceCooling
KSFA110A	3.1S	870°C • 9Hr OilQuenching & 600°C 17Hr AirCooling
KSFA110B	6.8S	870°C • 9Hr OilQuenching & 590°C 15Hr FurnaceCooling

Test specimens were cut out from round bar bulk materials having diameter of 320mm, and machined to hourglass type of shape with a minimum sectional diameter of 10mm. In the case of KSFA80A and KSFA110A, the test specimens were prepared which had a direction relative to the forged fiber flow of 0 degrees (referred to hereunder as being in the L direction), 45 degrees (referred to hereunder as being in the S direction) and 90 degrees (referred to hereunder as being in the T direction), while the test specimens of KSFA80B and KSFA110B were prepared which were in the L and T directions, respectively. Because the Vickers hardness distribution at a section of the bulk materials were almost constant from the surface to the center as shown in Fig. 1, the test specimens were cut out from each position of bulk materials including the center.

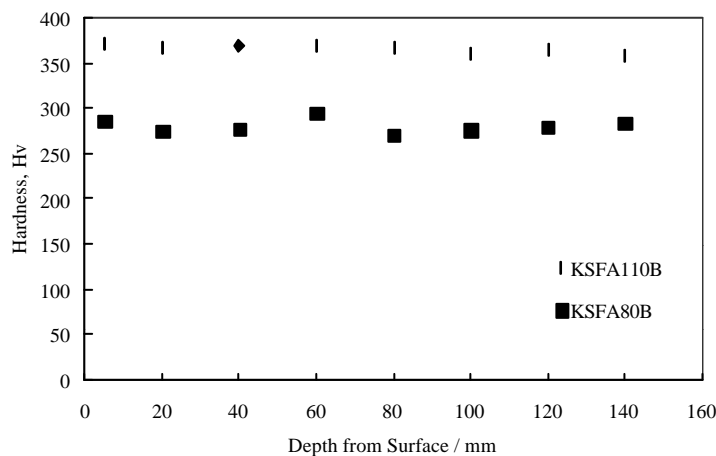


**Figure 1:** Vickers hardness of bulk materials, KSFA80B and KSFA110B

Fatigue tests were carried out on the test specimens using a canti-lever type rotational fatigue testing machines at 3,000rpm of rotating speed. Detailed observations of the fracture surfaces of each specimens were made using scanning electron microscope (SEM) and energy dispersive X-ray analyzer (EDX) thereby identifying inclusions that were the crack origin of fatigue fracture.

## EXPERIMENTAL RESULTS

### S-N properties

S-N diagrams of each sample material are shown in Figs. 2 and 3. In these figures, different plot symbols were used to indicate whether the fatigue crack started at the surface of test specimen (surface fracture) or at the interior of test specimen (interior fracture). Surface fracture means fatigue crack started at slip band or at a surface inclusion, and interior fracture means fatigue crack started at an interior inclusion. In Fig. 4, "f" mark was added to the plots for fish eye type fracture.

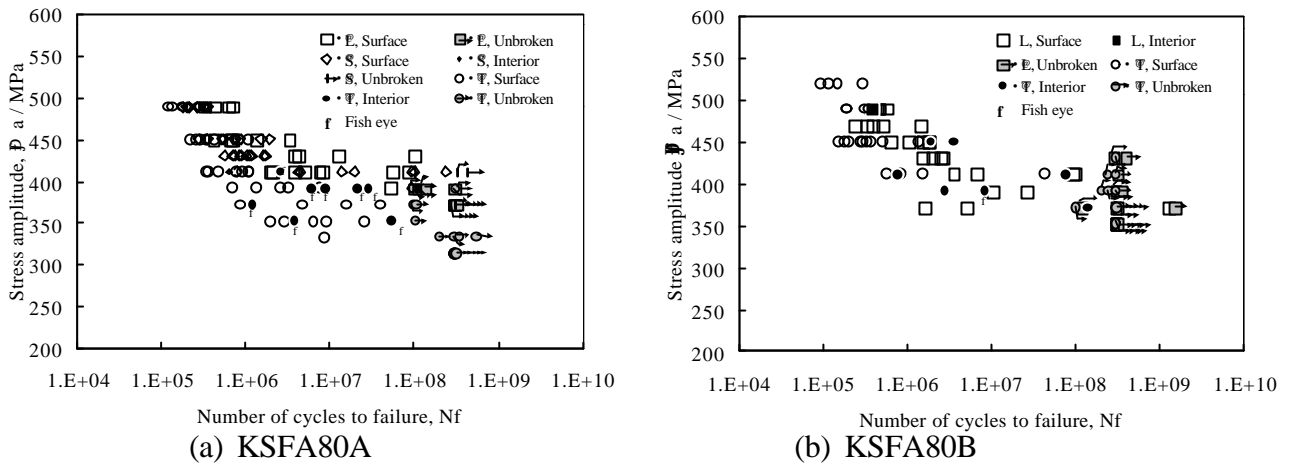


Figure 2: S-N diagrams of KSFA80

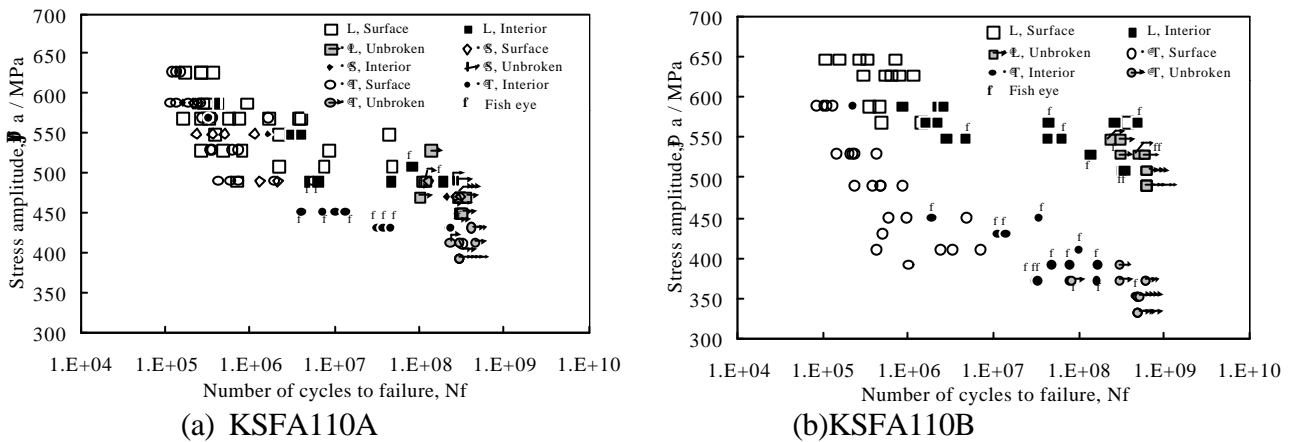


Figure 3: S-N diagrams of KSFA110

The fatigue strength of KSFA80A, KSFA110A and KSFA110B in the T direction are lower than those in the L direction, namely, the anisotropy of fatigue strength appears clearly. This tendency is the most remarkable in KSFA110B. On the other hand, the fatigue strength of KSFA80B in the L direction and the T direction show almost equal values. The fatigue strength of KSFA80A and KSFA110A in the S direction are slightly lower compared with those in the L direction, but in the long fatigue life range, there seems no significant difference between them. As shown in Figs. 2 and 3, fatigue fractures occurred at even more than  $10^7$  cycles of repeated stress which generally regarded as fatigue limit, and most of these fatigue fractures started at an interior inclusion. This type of fracture is more remarkable in KSFA110 than KSFA80. Fatigue fractures starting at an interior inclusion in the long life range are reported in many papers [1,2] recent years in steels with an extremely high tensile strength like bearing steel (about  $\sigma_B=2,000\text{MPa}$ ), but there seems no previous study using low alloy steel with the strength of the same level as the sample materials in this study. The above experimental results suggest that the interior fatigue fracture in the long life range occurs in steels having a tensile strength of more than 800MPa.

### Effect of inclusion to fatigue strength

As described above, there is a tendency that fatigue fracture starts at an interior inclusion in the long life range in high strength low alloy steels, but the mechanism of that interior fatigue fracture has not completely clarified by now. As for the present experiment, compressive residual stress was confirmed in the surface thin layer of the test specimens using X-ray stress measurement method. This compressive residual stress is thought to be one of the causes of the interior fatigue fracture.

This compressive residual stress exists in the surface hardening layer introduced by grinding when test specimens were machined. It takes the maximum absolute value of 400MPa at specimen surface and decreases to 0MPa roughly at a depth of 50 $\mu$ m (see Fig. 4).

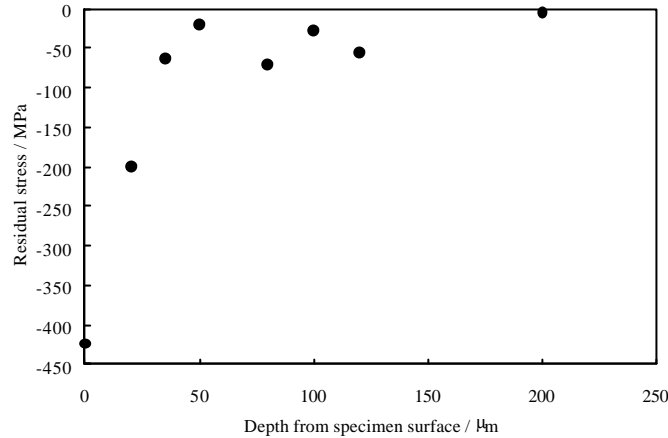
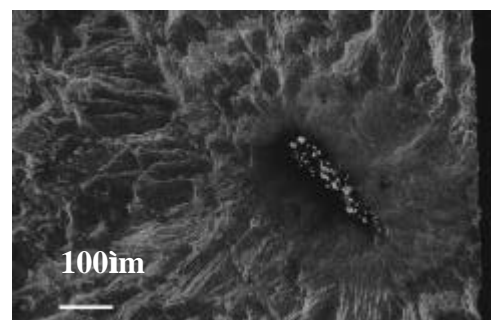
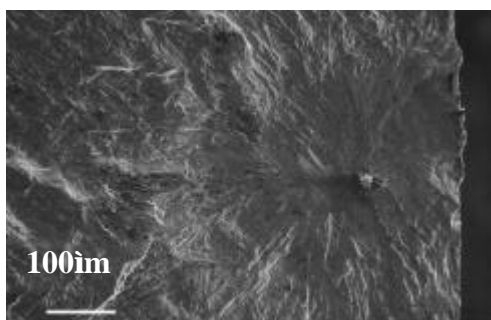


**Figure 4:** Residual stress distribution of test specimen (KSFA80B)

However, most of the surface inclusions of specimens in the T direction are much longer than the depth of the region where residual stress exists, therefore, it is difficult to explain the mechanism of the interior fatigue fracture only by the influence of the surface hardening layer. As another factor of the interior fatigue fracture, the difference of environment between the surface and the interior is assumed. For example, crack closure caused by oxidation takes place only at the surface. Moreover, the effect of hydrogen embrittlement around interior inclusions was proposed in a recent study [3]. To clarify the mechanism of the interior fatigue fracture, a quantitative examinations of these factors are necessary in the future.

Fig. 5 shows Two examples of SEM images of fatigue crack origins. These are fracture surfaces of the specimens fractured in the long life range, and fish eye type fractures are observed. The inclusion shown in Fig. 5(a) is observed at KSFA110B in the L direction, which has circle shape on the fracture surface. On the other hand, the inclusion shown in Fig. 5(b), observed at KSFA110B in the T direction, has thread-like shape on the fracture surface. The latter is clusters of many small inclusion grains. From EDX analysis, the inclusions at crack origins are mostly composed of Mg, Al, Si and Ca, and assumed to be an oxide type, while some MnS were also observed.



(a) KSFA110B-L ( $\sigma_i=568$ MPa,  $N_f=43,655,200$ ) (b) KSFA110B-T ( $\sigma_i=372$ MPa,  $N_f=30,825,250$ )

**Figure5:** SEM images at crack origins

Table 3 shows the values of average and standard deviation of sizes of inclusions at crack origins,  $a$ ,  $b$ ,  $(a+b)/2$  and  $a/b$ , where  $a$  is a length of short side of circumscribed rectangular of the inclusion and  $b$  is a length of long side of the rectangular.

**TABLE 3**  
AVERAGE VALUES OF SIZE AND ASPECT-RATIO OF INCLUSIONS

Mater.	Number of inc.	Size ( $\mu\text{m}$ )						Aspect -ratio	
		$a$		$b$		$(a + b) / 2$		$(a / b)$	
		Ave.	Std. dev.	Ave.	Std. dev.	Ave.	Std. dev.	Ave.	Std. dev.
80A-L	0	-	-	-	-	-	-	-	-
80A-S	11	<b>26</b>	12	<b>57</b>	41	<b>42</b>	25	<b>0.5</b>	0.2
80A-T	34	<b>37</b>	16	<b>295</b>	203	<b>166</b>	104	<b>0.2</b>	0.1
80B-L	9	<b>44</b>	24	<b>56</b>	27	<b>50</b>	25	<b>0.8</b>	0.2
80B-T	25	<b>51</b>	21	<b>69</b>	38	<b>60</b>	25	<b>0.8</b>	0.2
110A-L	27	<b>35</b>	14	<b>45</b>	17	<b>40</b>	14	<b>0.8</b>	0.2
110A-S	14	<b>34</b>	13	<b>67</b>	33	<b>51</b>	18	<b>0.6</b>	0.3
110A-T	29	<b>38</b>	13	<b>161</b>	122	<b>100</b>	61	<b>0.4</b>	0.3
110B-L	23	<b>21</b>	6	<b>34</b>	15	<b>27</b>	9	<b>0.7</b>	0.2
110B-T	34	<b>49</b>	14	<b>352</b>	182	<b>201</b>	93	<b>0.2</b>	0.1

In each material except for KSFA80B, inclusions have thread-like shapes running in the direction of forging, and average values of  $a/b$  are about 0.2-0.4 in the T direction specimens and are about 0.7-0.8 in the L direction specimens. Inclusions of KSFA80B have nearly circle shape on the fracture surface both in the L and the T direction specimens, and their average values of  $a/b$  are both 0.8. The anisotropy of the fatigue strength of each sample material appeared in the S-N characteristics of Figs. 2 and 3 depends on three-dimensional shapes of inclusions, and was remarkable in steels containing thread-like shape inclusions. For convenience, assuming  $(a+b)/2$  is a representative value of projected size of inclusion on the fracture surface, there is a tendency that the fatigue strength decreases as the average value of the size of inclusion becomes large.

Because the fatigue strength of steels depend on the size of inclusion at crack origin as mentioned above, It is expected that the fatigue strength could be estimated by the use of a parameter which combines stress with the size of the inclusion at crack origin, like initial stress intensity factor of micro crack initiated at the inclusion. Murakami et al [4,5] assumed proportional relationship between threshold stress intensity factor range of crack propagation,  $DK_{th}$  and cubic root of crack size,  $(area)^{1/3}$  and proposed a method called *area* parameter model for estimation of fatigue limit as equations (1) .

$$S_w = \frac{F(H_v + 120)}{(\sqrt{area})^{1/6}} \quad (1)$$

Where  $S_w$  - fatigue limit (MPa),  $H_v$  - Vickers hardness (kgf/mm<sup>2</sup>)

$area$  - Square root of projected area of inclusion ( $\mu\text{m}$ )

$F$  - Shape parameter

=1.43 for surface inclusion

=1.56 for interior inclusion

Fig. 6 shows a relationship between  $S_u/S_w$  and  $N_f$ , where  $S_u$  is stress amplitude and  $S_w$  is estimated fatigue limit calculated from equation (1) corresponding to the size of each inclusion observed at crack origin. For the calculation of  $S_w$ ,  $area$  values were represented by ellipse for interior inclusions and by semi-ellipse for surface inclusions. As for extremely long inclusions,  $area$  values were of the ellipse which semimajor axis is five times of semiminor axis uniformly [6]. The values of Vickers hardness used for calculations were the average values of the measurement results shown in Figure 1. For each sample material, all the values of  $S_u/S_w$  are above 1.0 except for one of KSFA110B. This means that almost all the specimens broke at higher

stress amplitude than estimated fatigue limits. And the difference between the lowest estimated value,  $S'_w$  and applied stress amplitude,  $S_i$  for each material is within 10% of  $S_i$ . From these results, it is recognized that the equations (1) can estimate fatigue limits of forged low alloy steels approximately. As well as KSFA80B, almost same  $S_i/S'_w$  values are obtained for both in the L and the T direction in KSFA110B of which sizes of inclusions,  $area$  are largely different from each other. Displayed by "x" or "+" mark in Fig. 6(a) are data of unbroken specimens at  $3 \times 10^8$  cycles of repeated stress. The  $S_i/S'_w$  values of these unbroken specimens were calculated using  $area$  of the inclusions observed at the crack origins on the compulsorily fractured surfaces. It is reasonable that these values of unbroken specimens were almost the minimum values in all data obtained in KSFA80B.

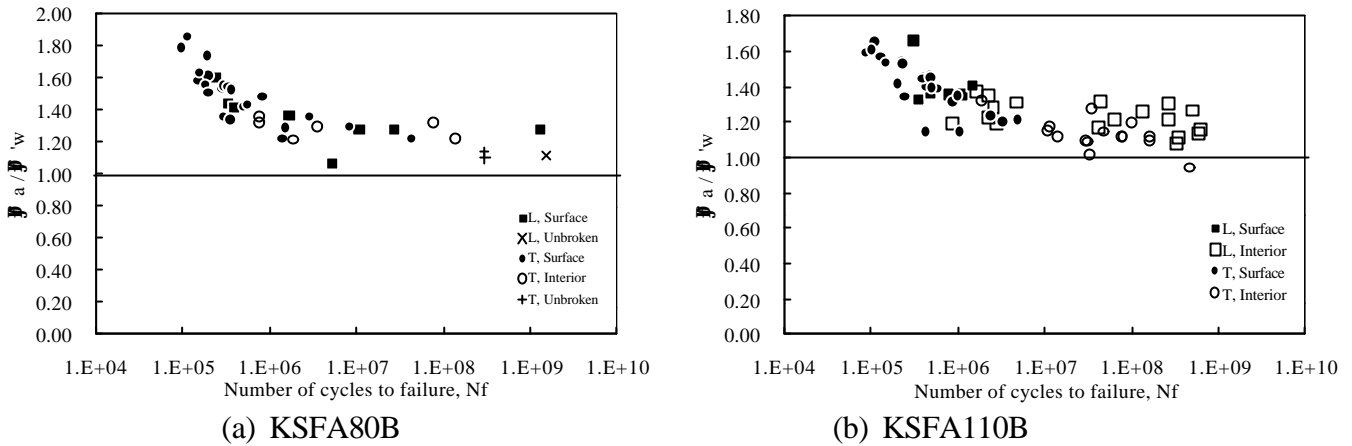


**Figure6:** Relationship between  $S_i/S'_w$  values and  $N_f$

From the above experimental results and considerations, it was shown that the fatigue strength of forged steels were affected by the shape and the size of inclusions and the anisotropy of fatigue strength of forged materials were explained by this. Therefore, it is clear that the most effective way to improve the fatigue properties of forged steel is to make the inclusions spherical and small.

## CONCLUDING REMARKS

The experimental findings and the conclusions drawn from the present study are summarized as follows.

- (1) Most of the inclusions at crack origins are oxidants composed of Mg, Al, Si and Ca, and even very small inclusion about  $10\mu\text{m}$  acts as fatigue crack origin.
- (2) In the long life range, fatigue crack initiates at an interior inclusion in high strength low alloy steel.
- (3) Three-dimensional shape and size of inclusions in steel affect fatigue strength, and the anisotropy of forged material can be explained by this. The most effective way to improve the fatigue properties of forged steel is to make the inclusions spherical and small.
- (4) Using the  $area$  parameter model, fatigue limit of forged low alloy steel can be approximately estimated.

## REFERENCES

1. Shiozawa, K., Lian-Tao, L. and Ishihara, S. (1999). *J. Soc. Mater. Sci. Jpn.* 48, 10, pp.1095-1100
2. Nishijima, S. and Kanazawa, K. (1999). *Fatigue Fract. Eng. Mater. Struct.* 22, pp.601-607
3. Murakami, Y., Nomoto, T. and Ueda, T. (1999). *Fatigue Fract. Eng. Mater. Struct.* 22, pp.581-590.
4. Murakami, Y. (1993). *Metal fatigue: effects of small defects and non-metallic inclusions*. Yokendo Ltd., Tokyo.
5. Murakami, Y., Takada, M. and Toriyama, T. (1998). *Int. J. Fatigue.* 16, 9, pp.661-667.
6. Murakami, Y and Endo, M. (1983). *Trans. Jpn Soc. Mech. Eng., Ser. A.* 49, 438, pp.127-136